Jurnal Kejuruteraan 36(3) 2024: 1187–1198
https://doi.org/10.17576/jkukm-2024-36(3)-28

Effect of Welding Parameters on Lap Shear Force of Similar and Dissimilar Friction Stir Spot Welded Aluminium Alloys

(Kesan parameter kimpalan terhadap daya ricih tindih kimpalan bintik kacau geseran bagi aloi aluminium serupa dan tidak serupa)

Ahmed Esmael Mohan[a,c], Zainuddin Sajuri[a,b*], Amir Hossein Baghdadi[a], & Nashrah Hani Jamadon[a,b]

[a]*Department of Mechanical and Manufacturing Engineering, Faculty of Engineering and Built Environment, Universiti Kebangsaan Malaysia, 43600 UKM Bangi, Selangor, Malaysia*

[b]*Centre for Materials Engineering and Smart Manufacturing, Faculty of Engineering and Built Environment, Universiti Kebangsaan Malaysia, 43600 Bangi, Selangor, Malaysia.*

[c]*Technical College of Al-Musaib, Al-Furat Al-Awsat Technical University, Kufa, Iraq*

[*]*Corresponding author e-mail: zsajuri@ukm.edu.my*

Received 11 November 2023, Received in revised form 7 February 2024
Accepted 3 March 2024, Available online 30 May 2024

ABSTRACT

Friction stir spot welding (FSSW) is a solid-state single-point welding technique that uses a rotating tool consisting of a shoulder and a pin for joining nonferrous metals and alloys. FSSW produces a keyhole at the welding point, which decreases the mechanical strength of the joints. This study investigates the influences of tool rotational speed (1000, 1250, and 1500 rpm) and dwell time (5, 10, and 15 s) on the shear fracture load of the FSSW joints. Two different grades of aluminium alloy plates, i.e., AA6061 and AA7075 were used to produce similar (7075-7075 and 6061-6061) and dissimilar (6061-7075) alloy joints. The plates with a thickness of 3 mm were folded above each other before a rotating tool pin was plunged through the thickness of the top plate to obtain an FSSW lap joint. It was found that tool rotational speed and dwell time induced a considerable impact on the microstructure, and shear strength. The results indicated that the grain size of microstructure in similar and dissimilar joints was affected by the rotational speed and dwell time. The grain size of the microstructure increased as rotational speed and dwell time increased. The results also showed that a tool rotational speed of 1250 rpm and dwell time of 10 s gave the highest shear fracture load for 7075-7075 similar and 6061-7075 dissimilar joints. However, for 6061-6061 similar joints, the highest mechanical strength was obtained at 1250 rpm and 10 s.

Keywords: Friction stir spot welding; Rotational speed; Dwell time; Fracture load; Aluminium alloys

INTRODUCTION

Aluminium (Al) and its alloys are excellent light metals, used in aerospace, marine and automotive structures for their high mechanical capacity, strong resistance, and corrosion resistance (Baghdadi et al. 2019; Paidar et al. 2020). 6061 and 7075 Al alloys are among the top materials used in these industries. 6061 Al alloy is used more frequently relative to 7075. This is because 6061 is more cost-effective, of medium strength, and has good weldability and formability. Whilst 7075 Al alloy is exceptionally strong with typically smoother finishes but more costly. For structural components such as aircraft wings and panels, high-strength 7075 Al alloys are always used (Liu et al. 2019). Furthermore, 6061 Al alloy is widely used as a major structural alloy in many industries, including light-rail transits and high-speed train bodies (Liu et al. 2019). Obtaining a 7075/6061 joint with satisfactory mechanical properties is essential. Al alloys are difficult to join using traditional fusion welding processes (Rodriguez et al. 2015) due to difficulties such as fracture and crack formation, residual stress, and fracture

solidification (Gibson et al. 2014; Rodriguez et al. 2015).

Friction stir welding (FSW) was discovered in 1991 to combine a wide range of metals, especially magnesium (Mg) and aluminium (Al) alloys (Mamgain et al. 2023; Pabandi et al. 2018). The maximum temperature obtained in the FSW process is usually less than the melting temperature of the base material (Baghdadi et al. 2022). However, joining in a solid-state condition is possible in the FSW process by stirring the plasticised material of the welded materials because generated of the frictional heat by a rotating tool to join materials. Numerous researches have been carried out to understand the metal and mechanical behaviour of FSW joints (Buffa et al. 2013; Yan et al. 2016). In 2001, automotive manufacturers began using the FSSW technique to replace resistance welding of aluminium alloys (Paidar et al. 2015, 2020; Paidar & Sarab 2016) that in many cases resulting in weaker weld seam and porosity formation(Wang & Lee 2007; Su et al. 2014). The metal and mechanical properties of FSSW welded specimens were noted as excellent, but a tool-induced opening in the joint is inevitable (Paidar et al. 2020). In the FSSW process, tool design is very important where the non-consumable tool with pin and shoulder are rotating at high speed and gradually placing them on overlapping sheets (Asmael & Glaissal 2020; Liu et al. 2019). Plunging, stirring, and retracting are three separate processes that make up the FSSW process. The method starts with a high-speed rotation of tool and gently plunging it into two sheets that overlap at a single point till the shoulder touches the upper surface of the plate. The anvil under the lower plate is utilized to maintain the axial force of the tool at the same time. Subsequently, a certain period (usually in seconds) is maintained to mix the two metal sheets. Finally, once the rotating tool is removed from the workpiece (Badarinarayan et al. 2009; Mitlin et al. 2006; Yazdipour & Heidarzadeh 2016), a solid-state bond forms at the interface between the top and bottom plates, as depicted in Figure 1.

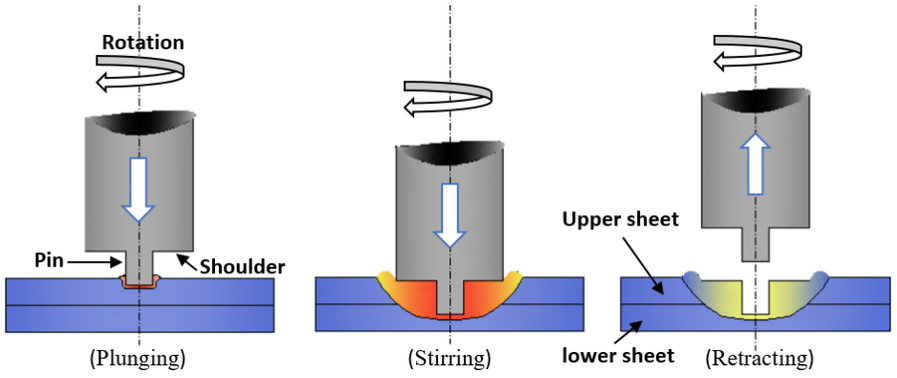

FIGURE 1. FSSW process diagram.

The influences of two important welding parameters, i.e., tool rotational speed (RS) and dwell time (DT), have been reviewed. For instance, Hunt et al. (2006) noted that the increasing DT leads to an increase in joint strength. Tran et al. (2008) stated that the strength of AA 5754-O and 7075-T6 FSSW increased with the increase of the DT. The study on high RS of the tool at 1000 to 2500 rpm was done by Aydın et al. (2021). The DT was set to 7 s, feed speed to 50 mm.min-1, and 5 mm depth of plunging to reach a 3 mm AA6082-T6 plate thickness FSSW joint. The results show that the hardness of the welded surface is less than that of the base material. Nasir et al. (2021) studied the influence of RS and DT on the microstructure and mechanical properties of FSSW joints of dissimilar aluminium plates (AA5754 - AA7075(T651)). It was observed that the shear fracture load at 1000 rpm, and 2 s, reached 8.063 KN. while it decreased by about 25% with a DT of 5 s at a RS of 1400 rpm. According to Zhang et al. (2011), the results of tension tests showed that the joint performance decreases as the RS increases. The highest tensile/shear resistance (2847.7 N) was attained in the welding condition at a RS of 1540 rpm and a DT of 5 s. In addition, Asmael and Glaissal (2020) also studied the mechanical properties and microstructure of the RS and DT of different aluminium and titanium alloy FSSW joints. They discovered that the maximum shear fracture load for 1000 rpm, and 10 s was about 4.2 kN. Shen et al. (2013) stated that the friction stir-spot welds from 6061-T4 aluminium alloys were affected by processing variables of RD (1200, 1500, 1800, 2100 rpm) and DT (2, 4 s). They found that when the RS was 2100 rpm and DT was 4 s, the tensile shear strength reached a highest of 2125 N.

According to Garg and Bhattacharya (2017), the increase in RS reduced the lap shear force, but the DT of

the FSSWed AA6061 alloy increased and then decreased the lap shear force. They noted that the ideal tool rotation parameters were 1000 rpm, 4 s of DT, and square tool pin shape with a thickness of 3860 N. They also discovered that the RS had the greatest impact on mechanical properties, followed by the shape of tool pin and DT. Sekhar et al. (2018) examined the influence of the RS of the FSSWed AA5052-H38 tempered at different rotational speeds of 500 rpm to 1300 rpm. They pointed out that the force of lap shear force increased as tool RS increase from 500 to 900 rpm, and then decreased with the further increase in tool RS. The maximum load of the failure of the tensile shear was 4.215 kN. Lee et al. (2017) examined the joint strength and microstructure development of AA6061T6 friction stir-pot welding using process variables such rotational speed (800, 1000, 1500 rpm), dwell time (1, 2, 3, 4, 5, and 6 s) and tool pin angle. They found the maximum joint resistance was 2.78 kN at 1000, 1500 rpm, and 5s. Ahmed et al.(2022) carried out a study in which they examined the welding of thin AA6082-T6 sheets, with thicknesses of 1 mm, and 2 mm, using FSSW. They investigated various RS (400, 600, 800, and 1000 rpm) while maintaining a consistent dwell time of 3 s. Their research revealed that a RS of 600 rpm resulted in the highest lap shear force of 4.3 kN.

All previous studies have demonstrated that FSSW has a good potential for joining aluminium alloys. However, to accomplish proper welding, adequate welding parameters and types of material must be carefully examined, especially for similar and dissimilar alloys. Hence, the continuous improvement of the joint properties is critical. The aim of this study is to investigate the influences of RS and DT on the microstructure, and shear fracture load of the FSSW joints. In this study, FSSW is applied to both similar (AA7075-AA7075 and AA6061-AA6061) and dissimilar (AA6061-AA7075) joints in a lap joint arrangement.

METHODOLOGY

EXPERIMENT DESIGN AND PROCEDURE

In this study, AA6061 and AA7075 aluminium alloys sheets were used as the base materials. Table 1 displays the composition and mechanical characteristics of these alloys.. Samples with the size of 100 × 25 × 3 mm^3 have been considered in similar and dissimilar welding processes of AA6061 and AA7075 and an overlap area of 25 mm × 25 mm as shown in Figure 2(c). The FSSW process used a 4 mm long and 15 mm shoulder diameter cylindrical threaded M5 pin. The pin is made of H13 steel and was heat-treated to a hardness of 53 to 55 HRC. The pin used and its dimension is illustrated in Figure 1 (a).

Figure 2(b) shows the welding configuration of the similar and dissimilar materials lap joint. Three different configurations were prepared, namely AA6061-AA6061, AA7075-AA7075 (similar) and AA6061-AA7075 (dissimilar) joints. Prior to welding, the surface of the sheet was cleaned with steel brushes to remove the oxide layer and then cleaned with ethanol.

TABLE 1. Chemical composition and mechanical characteristics of the alloys utilised in this research.

Alloy	Chemical composition (wt.%)						Yield strength [MPa]	Ultimate Tensile [MPa]	Elongation [%]
	Al	Mg	Si	Cu	Zn	Fe			
AA6061	Bal	1.00	0.81	0.3	0.02	0.21	298	342	16.9
AA7075	Bal	2.5	0.2	1.93	6.08	0.46	542	587	9.6

The effects of RSs (1000, 1250, and 1500 rpm) and DT (5, 10 and 15 s) on mechanical characteristics of the FSSWed Al alloys were investigated. Optical microscopy (OM) was utilised to examine the microstructure of the samples. To analyse the microstructure, specimens were prepared, ground, polished, and then immersed in an etching solution composed of 1 ml of hydrofluoric acid, 2.5 ml of nitric acid, 1.5 ml of hydrochloric acid, and 95 ml of distilled water for about 30 seconds. The lap-shear tensile strength has been analyzed according to the 17.2 standard of the American Welding Association (AWS), and the specimen configuration is depicted in Figure 3(b) (AWS, 2013). Tensile tests were conducted at room temperature using a Zwick Roell universal test machine with capacity of 100 kN. The crosshead speed was set constant at 1 $mm.min^{-1}$. The shear failure load of each specimen was calculated as the average of three measurements.

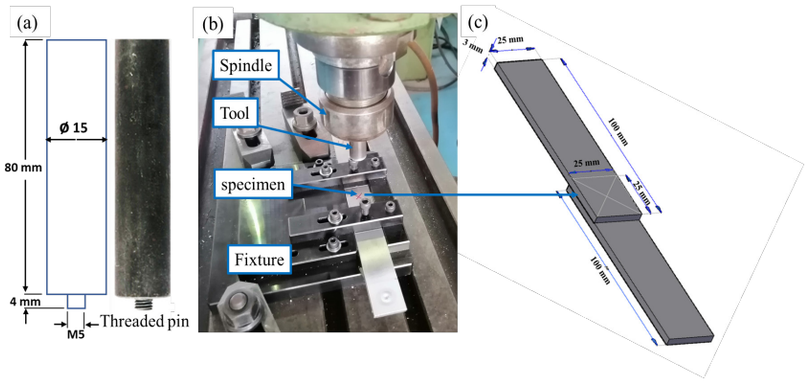

FIGURE 2. Set-up of the experimental welding and tensile test

RESULTS AND DISCUSSION

MICROSTRUCTURE ANALYSIS

The microstructure analysis of the FSSW joint involves the use of an optical microscope to examine granular alterations and to detect imperfections such as voids, inclusions and cracks that may occur after welding. Figure 3 illustrates the cross section of the FSSW joint. In all welding categories of the FSSW, the welding tool creates pinhole by cylindrical pin. In particular, the region near this pinhole and the area below the shoulder represent the regions that are subject to the primary thermal input and material flow. It is worth mentioning that studies have indicated that over 70% of the heat input generated through friction during the process of welding is attributed to the bottom of the tool's shoulder area (Akbari et al. 2016; Ojo et al. 2015).

With this understanding, the material adjacent to the tool's shoulder surface experiences significant levels of heat input, shear, and compression deformation. Consequently, the widest size of the stir zone (SZ) is found around the tool's shoulder, and in this study, the SZ area is defined as the width observed in all joints. Therefore, the SZ width of the joints (as shown in Figure 3) is measured to numerically clarify the influence of different parameters on the SZ width. The width of the SZ is expanded when the RS and the DT increase from 1000 to 1500 rpm and 5 to 15 s respectively, as shown in Figure 3. This phenomenon is due to an increase in friction-produced heat input, and volume of material flow from the shoulder area of the tool to the tip of the pin (Zhang et al. 2021). An increase in SZ width has also been reported (Bozzi et al. 2010; Zhang et al. 2021).

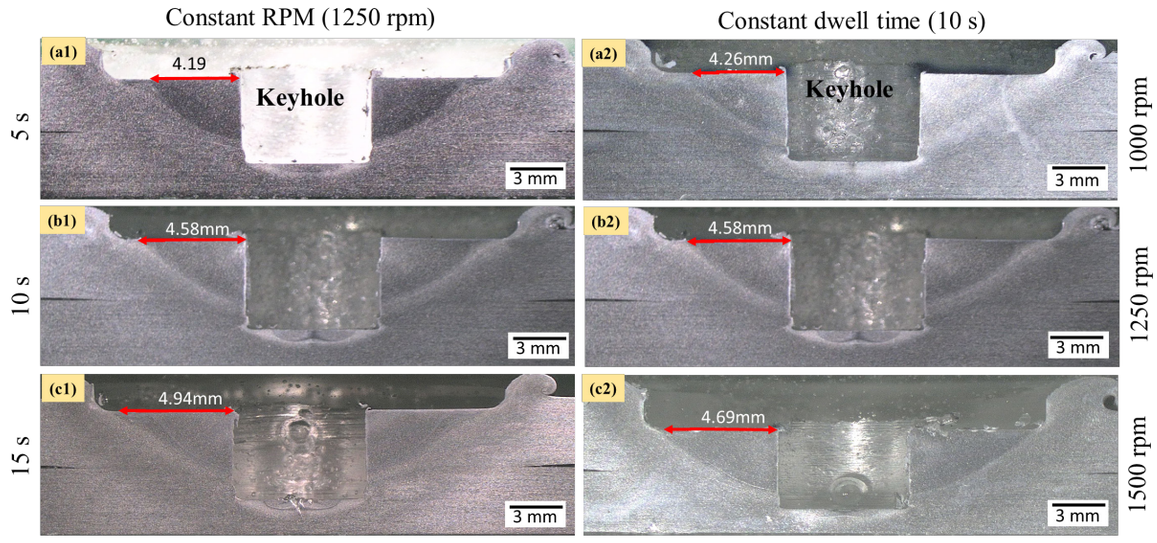

FIGURE 3. Cross-section view of SZ size of the similar joint of AA6061 at a constant RS 1250 rpm with dwell time of (a_1) 5 s, (b_1) 10 s, (c_1) 15 s, and constant DT with of rotational speed (a_2) 1000 rpm, (b_2) 1250 rpm, (c_2) 1500 rpm

However, by increasing the width of the SZ, the bonding surface between the top plate, and the bottom plate expands. Figure 4 shows macro-photos of the bond width of similar joints with AA6061. Figure 4(a1, b1, c1) shows the macro-photos of the joining cross-section of the similar joint of AA6061 welded at constant rotational speed of 1250 rpm. Figure 4(a2, b2, c2) also shows the macro-photos of the joining cross-section of the similar joint of AA6061 welded but at constant DT of 10 s. From this figure, it is noted that the joining width increased with increasing DT and RS. This phenomenon is due to higher tool RS and the longer DT, which produces more heat, improves material flow, and therefore produces larger binding regions (Aydin et al. 2014; Pathak et al. 2013; Wang et al. 2015). The increased joining width will increase the lap/shear strength of joint. Furthermore, it can be seen from the figure that the bonding width decreases when used at lower rotational speeds and shorter dwell times (especially at 1000 rpm and 5 s). Therefore, using very low rotational speeds and short stirring times can cause insufficient mixing of top and bottom plate materials, thereby reducing the bond width. This in turn can potentially result in a reduction in shear strength. According to previous results (Shen et al. 2013), the smallest bond width was observed with the lowest RS and DT.

Figure 5 illustrates the influence of FSSW process on the microstructure of the dissimilar joint at a RS of 1250 rpm and a 10 s DT. The microstructure in the SZ (Stir Zone) consists of fine, equiaxed grains resulting from frictional heat, and the intense plastic deformation that occurs during welding, as depicted in Figure 5a. Simultaneously, the base metal (BM) experiences substantial plastic deformation because of the stirring action and heat generated during Friction Stir Welding (FSW), leading to a dynamic recrystallization process within the material. This dynamic recrystallization significantly contributes to grain refinement in the microstructure of SZ (Khan et al. 2017; Selamat et al. 2018). The FSSW region was divided into three zones: the stir zone (SZ), the thermal mechanical affected zone (TMAZ), and the heat affected zone (HAZ) (Baghdadi et al. 2020; Zhang et al. 2011) as illustrated in Figure 5b.

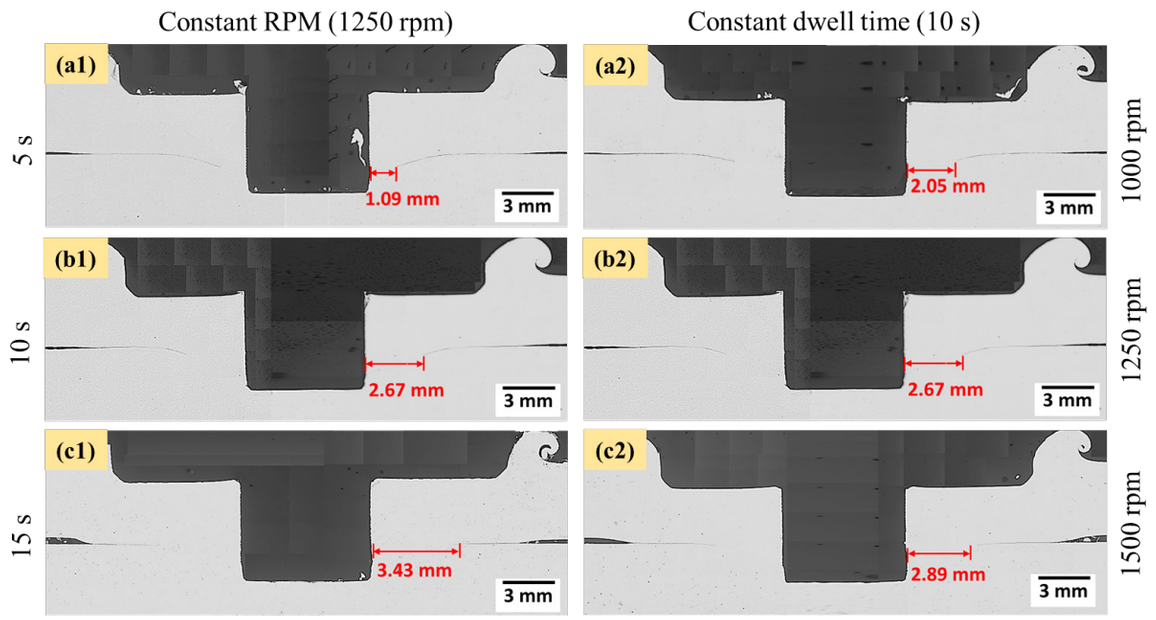

FIGURE 4. Cross-section view of the similar joint of AA6061 at constant rotational speed 1250 rpm with dwell time of (a_1) 5 s, (b_1) 10 s, (c_1) 15 s, and constant dwell time with of rotational speed (a_2) 1000 rpm, (b_2) 1250 rpm, (c_2) 1500 rpm

These zones are represented in Figure 5 as circular, oval, and triangular, respectively. Figures 6c-g display the high-magnification zones as the SZ, the TMAZ, the HAZ and the BM respectively. The average grain sizes (GS) of 42 and 73 µm were obtained for Al6061-BM and Al7075-BM, respectively.

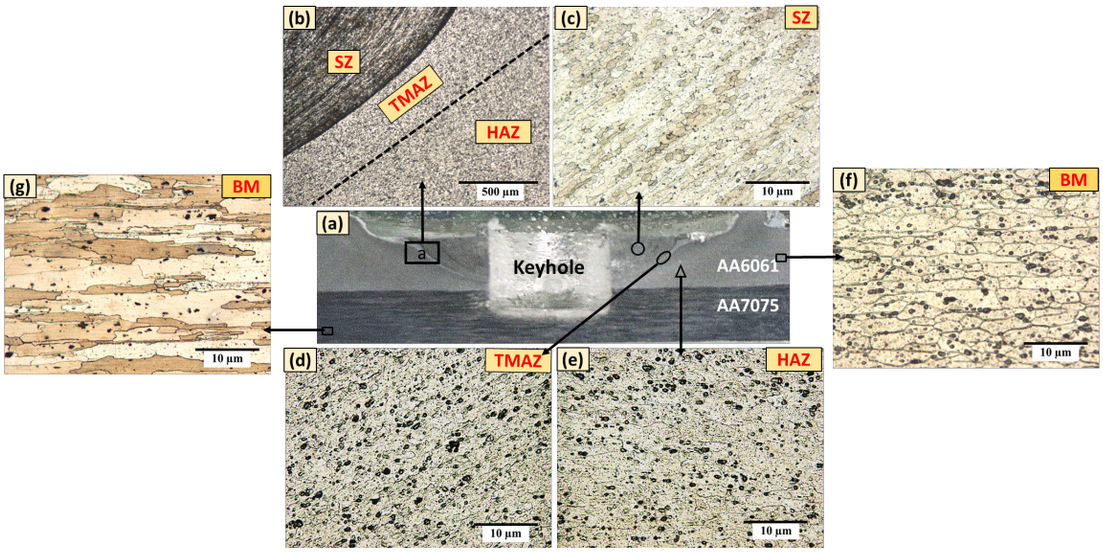

FIGURE 5. Microstructure of the dissimilar joint of AA6061-AA7075 at 1250 rpm and 10 s; (a) cross-sectional view, (b) SZ, (c) Weld Zone, (d) TMAZ, (e) HAZ, (f) AA6061-BM, and (g) AA7075-BM

Figure 6 displays the microstructures in the stir zone (SZ) of welded samples under varying conditions: RS of 1000 and 1500 rpm and DT of 5 and 15 seconds. Increased RS and DT resulted in the dissolution of precipitation-hardening particles. The figure illustrates that the SZ microstructures exhibited more recrystallized fine grains in comparison to the Base Metal (BM). It was noted that elevating both the RS and DT led to an increase in grain size, as depicted in Figure 6-8. The average GS of SZ of the AA6061 similar joint changed from 10 µm at 1000 rpm to 15 µm at 1500 rpm, for the SZ of the AA7075 similar joint the average GS varied from 7 µm at 1000 rpm to 11 µm at 1500 rpm and for the SZ of the dissimilar AA6061-AA7075 the average size varied from 11.5 µm at 1000 rpm to 15.5 µm at 1500 rpm. The increase in RS and DT results in an increase in thermal input, which led to an increase in the grain size in the SZ (Akbari et al. 2016; Baghdadi et al. 2022). An increase in average grain size was also reported (Ahmed et al. 2022).

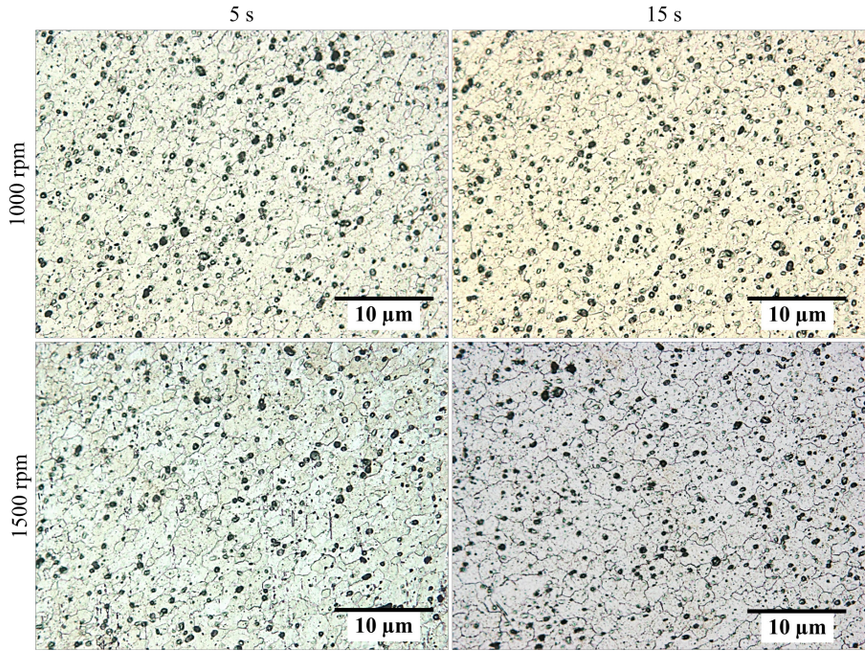

FIGURE 6. SZ microstructure images of the similar joint AA6061-AA6061

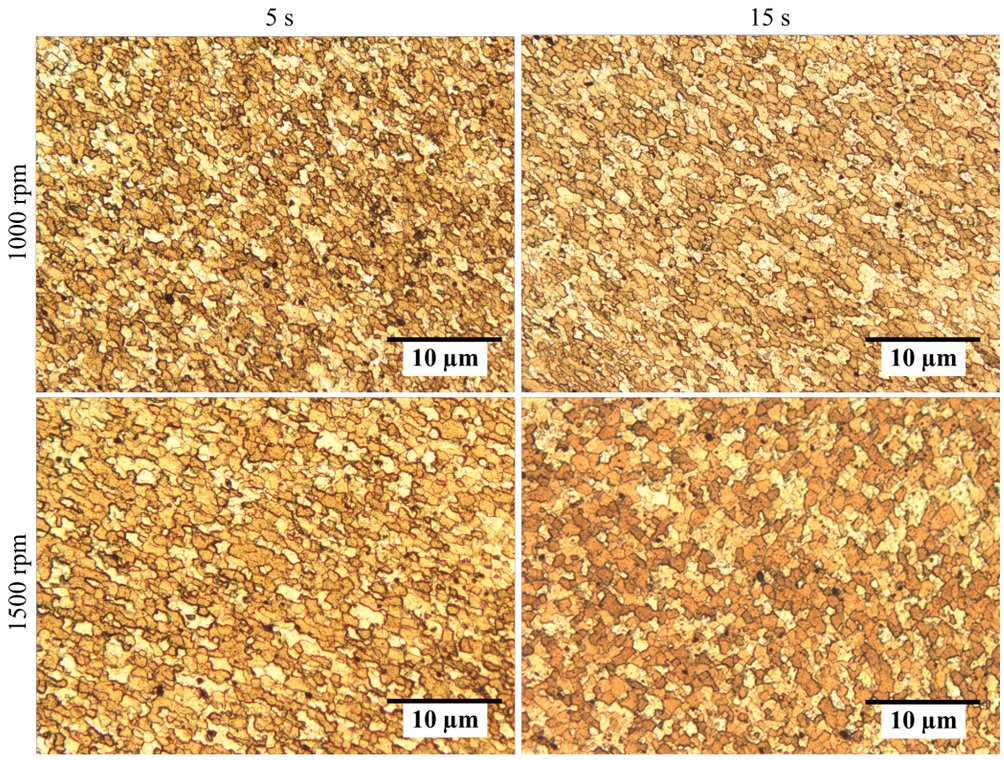

FIGURE 7. SZ microstructure images of the similar joint AA7075-AA7075

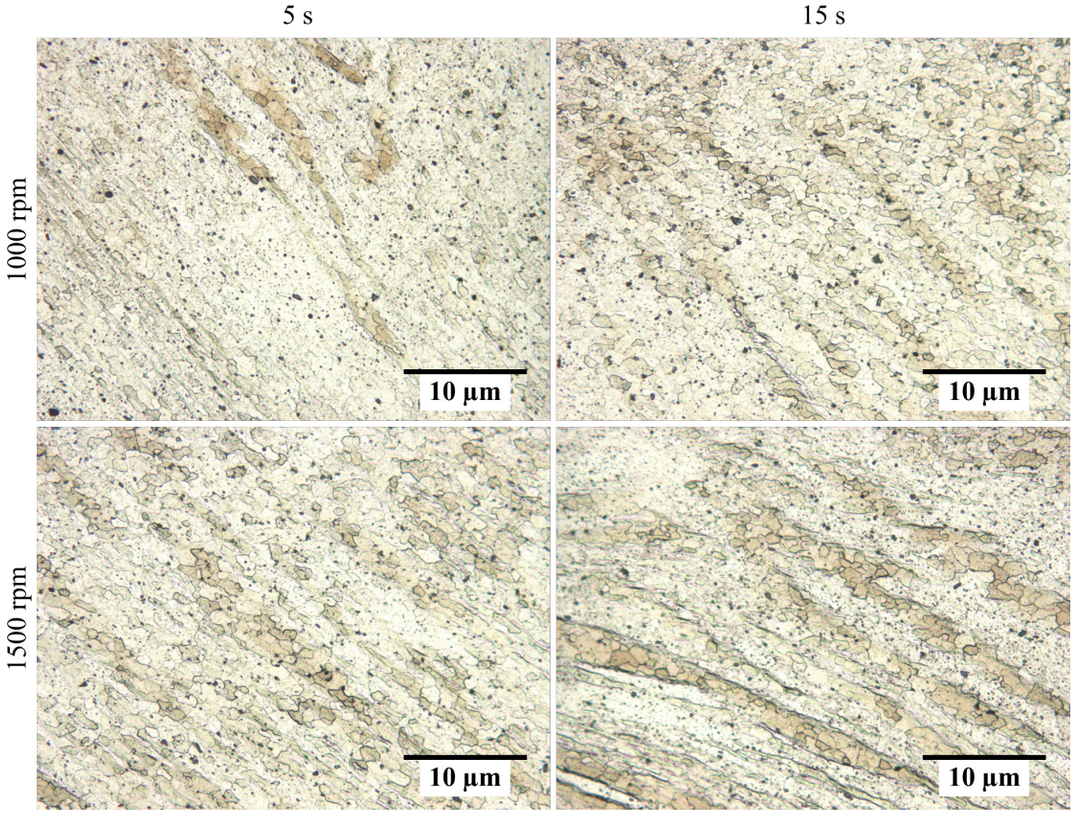

FIGURE 8. Microstructure images of the SZ of dissimilar joint AA6061-AA7075

The effect of various RS of 1000, 1250 and 1500 rpm on the microstructure of the TMAZ at constant dwelling of 10 s time is shown in Figure 9. The TMAZ experienced plastic deformation, although to a lesser extent than the SZ. In the TMAZ, grains were deformed, and elongated in the direction of rotation, mirroring the pattern observed in the SZ (see Figure 9). This area is influenced by thermal cycles and large plastic deformations caused by the interaction of tool and material in the welding process.

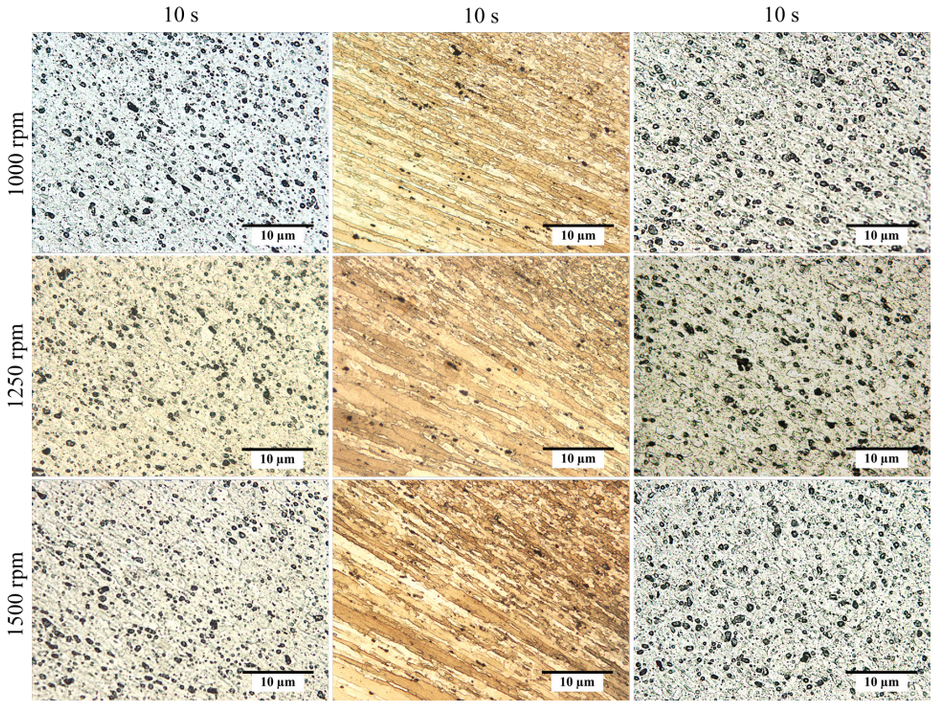

FIGURE 9. Microstructure images of the TMAZ of similar and dissimilar joint

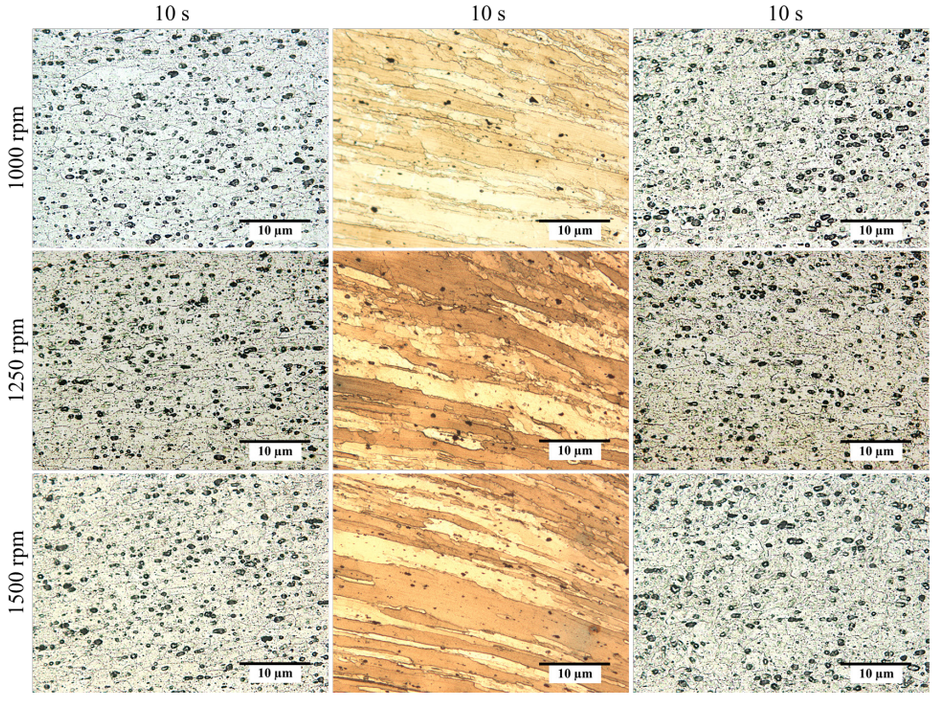

FIGURE 10. Microstructure images of the HAZ of similar and dissimilar joint

Moreover, The HAZ experienced heat treatment due to heat transfer from the SZ and the TMAZ. Consequently, the grain size in the HAZ was coarser than that of the TMAZ, as illustrated in Figure 10. The base metals (BMs) reached temperatures as high as 400 °C (Ilangovan et al. 2015), leading to an annealing effect. This annealing process resulted in the coarsening and dissolution of strengthening elements in the aluminum matrix. The HAZ underwent a thermal cycle due to an rise in temperature of up to 250 °C (Ataya et al. 2022). This temperature rise in the HAZ, driven by increased RS, likely contributed to the expansion of the average GS. Consequently, grain growth is expected will be observed compared to grain size of BM. Finally, the GS of the various welding zones (SZ, TMAZ, HAZ) is directly related to rotational speed, when the other process parameters are constant.

SHEAR FRACTURE LOAD

In the creation of new vehicle models, automotive engineers give top priority to evaluating the lap shear force performance of FSSWed joints. Consequently, every spot-welded joint produced undergoes rigorous tensile shear testing to guarantee its optimal performance. Recent studies have demonstrated that the welding process parameters play a pivotal role in influencing the tensile shear performance of these joints (Ataya et al. 2022; Pathak et al. 2013). For this reason, specific parameters, including dwell times of 5, 10, and 15 seconds, and three different RS of 1000, 1250, and 1500 rpm, were meticulously chosen for investigation.

Figure 11 presents the impact of dwell times and rotational speed on FSSWed joints of Al alloys, both for similar and dissimilar materials. At a constant rotational speed, the increase in DT from 5 to 10 s resulted in an increase in lap shear strength. In addition, it was observed that increasing RS and DT beyond 1250 rpm and 10 s led to a reduction in joint strength. This decline has been attributed to the elevated heat input generated at the interface of the tool, and workpiece at high rotational speed, along with the heat produced by severe plastic deformation, particularly at the SZ, which becomes trapped within the workpiece (Nasir et al. 2021). As a result, the adiabatic temperature effect causes uncontrolled growth of grain due to exposure to high temperatures for a long DT (Sadeghi et al. 2020; Zhang et al. 2011) as mentioned earlier (see Figure 6-8). However, when grain size increases, lap shear strength should decrease according to the Hall–Petch equation (Baghdadi et al. 2020). Furthermore, it was observed that the shear fracture load of spot lap joints decreased at process parameters of 1000 rpm and 5 s. This reduction in lap shear strength may be attributed to insufficient heat input, leading to inadequate mixing of metals during the process of welding for both similar and dissimilar joints, consequently resulting in a narrower joining width. Shen et al. (2013) also stated that the lowest RS and DT resulted in the smallest bonding width.

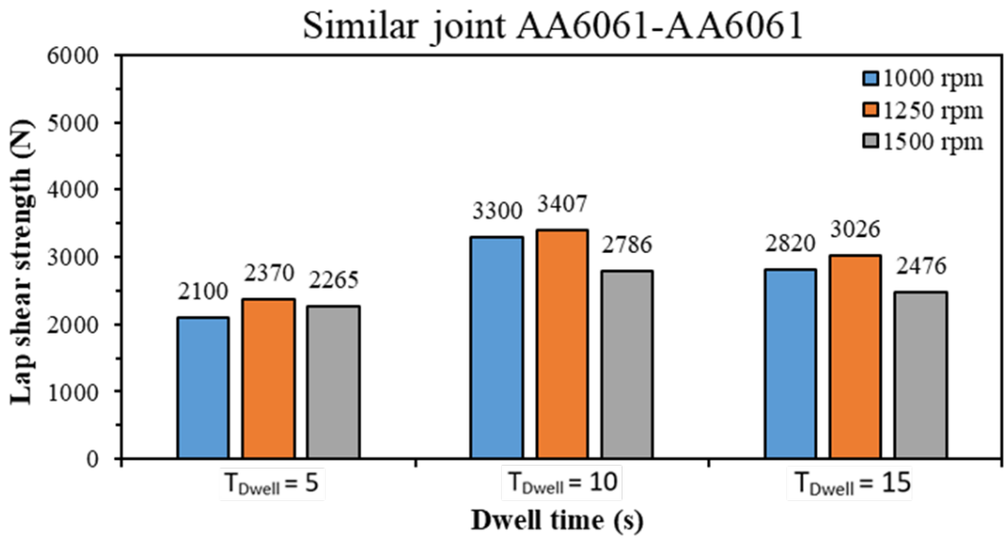

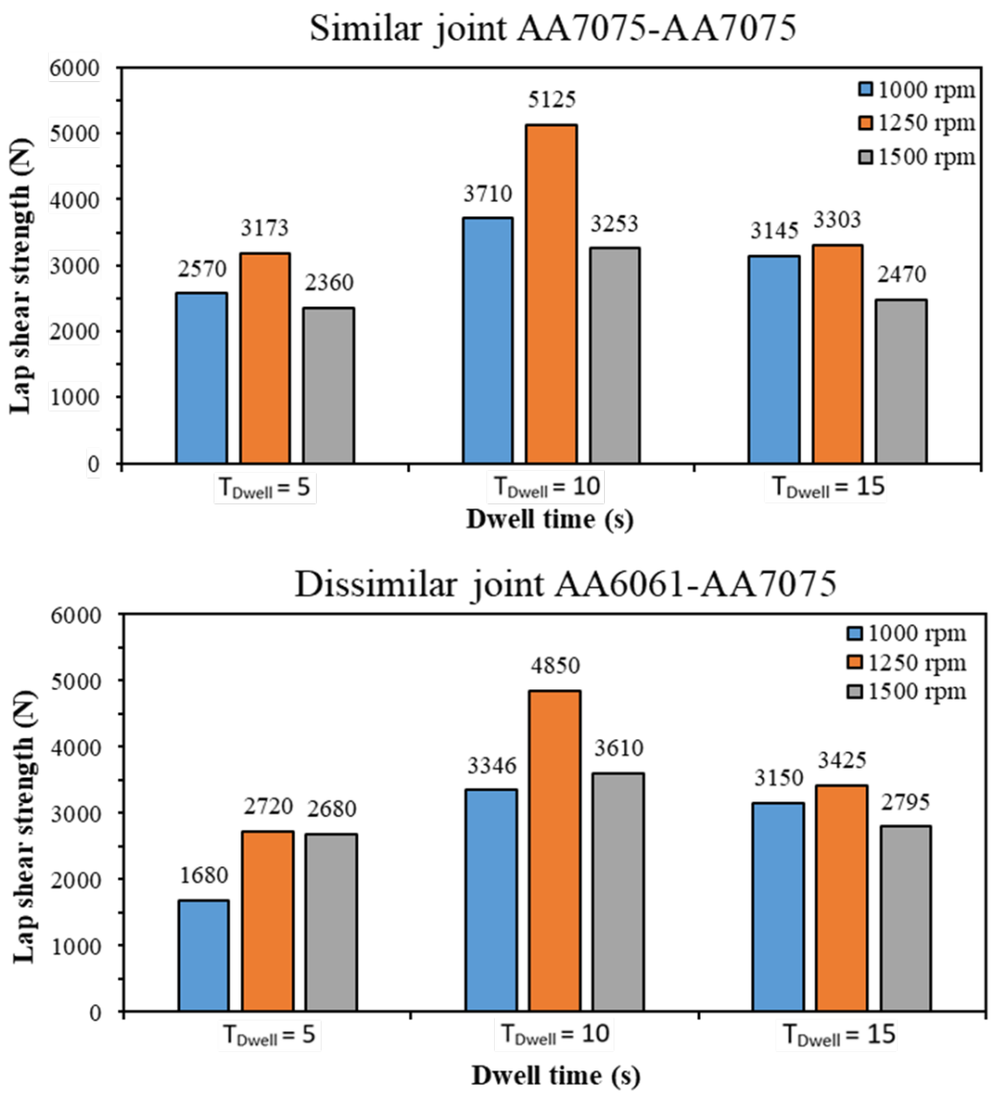

FIGURE 11. Lap shear strength of FSSWed samples at different welding parameters; Similar joint AA6061, AA7075 and Dissimilar joint AA6061-AA7075

CONCLUSION

Influence of RS and DT on the microstructure and shear fracture load of FSSW joints, similar AA6061, AA7075, and dissimilar AA6061-AA7075 joints have been investigated. The increase in RS and DT leads to the increase of metallurgically bonded zone and SZ. The GS in the various welding zones (SZ, TMAZ, HAZ) directly correlates with RS and DT. The highest shear fracture loads for 7075-7075 similar and 6061-7075 dissimilar joints were obtained for the joint made at a RS of 1250 rpm and DT of 10 s. However, for 6061-6061 similar joint, the highest mechanical strength was obtained at 1250 rpm and 10 s. Lower shear fracture loads for 7075-7075, 6061-6061 similar, and 6061-7075 dissimilar joints were obtained for the joint made at tool RS of 1000 and 1500 rpm and DT of 5s and 15.

ACKNOWLEDGEMENT

The authors would like to thank Universiti Kebangsaan Malaysia for their financial support under the grant DIP-2021-005.

DECLARATION OF COMPETING INTEREST

None

REFERENCES

Ahmed, M.M.Z., El-Sayed Seleman, M.M., Ahmed, E., Reyad, H.A., Touileb, K. & Albaijan, I. 2022. Friction stir spot welding of different thickness sheets of aluminum alloy AA6082-T6. *Materials* 15(9): 2971. DOI:https://doi.org/10.3390/ma15092971.

Akbari, R., Mirdamadi, S., Khodabandeh, A. & Paidar, M. 2016. A study on mechanical and microstructural properties of dissimilar FSWed joints of AA5251-AA5083 plates. *International Journal of Materials Research* 107(8): 752–761.

Amirhossein Baghdadi, Armin Rajabi, Nor Fazilah Mohamad Selamat, Zainuddin Sajuri & M.Z. Omar. 2019. Effect of post-weld heat treatment on the mechanical behavior and dislocation density of friction stir welded Al6061. *Materials Science and Engineering A* 754: 728–734.

Amirhossein Baghdadi, Zainuddin Sajuri, Azadeh Keshtgar, Nurulakmal Mohd Syarif & Armin Rajabi. 2022. Mechanical property improvement in dissimilar friction stir welded Al5083/Al6061 joints: Effects of post-weld heat treatment and abnormal grain growth. *Materials* 15(1): 288.

Amirhossein Baghdadi, Zainuddin Sajuri, M.Z. Omar & Armin Rajabi. 2020. Friction stir welding parameters: Impact of abnormal grain growth during post-weld heat treatment on mechanical properties of Al–Mg–Si welded joints. *Metals* 10(12): 1607.

American Welding Society. 2013. *AWS D17.2: Specification for Resistance Welding for Aerospace Applications*. AWS: United States of America.

Asmael, M.B.A. & Glaissa, M.A.A. 2020. Effects of rotation speed and dwell time on the mechanical properties and microstructure of dissimilar aluminum-titanium alloys by friction stir spot welding (FSSW). *Materialwissenschaft Und Werkstofftechnik* 51(7): 1002–1008.

Ataya, S., Ahmed, M.M.Z., El-Sayed Seleman, M.M., Hajlaoui, K., Latief, F.H., Soliman, A.M., Elshaghoul, Y.G.Y. & Habba, M.I.A. 2022. Effective range of FSSW parameters for high load-carrying capacity of dissimilar steel A283M-C/brass CuZn40 joints. *Materials* 15(4): 1–24.

Aydin, H., Tuncel, O., Yuce, C., Tutar, M., Yavuz, N. & Bayram, A. 2014. Effect of rotational speed and dwell time on mechanical properties of dissimilar AA1050-AA3105 friction stir spot welded joints. *Materials Testing* 56(10): 818–825.

Aydın, H., Tunçel, O., Tutar, M. & Bayram, A. 2021. Effect of tool pin profile on the hook geometry and mechanical properties of a friction stir spot welded AA6082-T6 aluminum alloy. *Transactions of the Canadian Society for Mechanical Engineering* 45(2): 233–248.

Badarinarayan, H., Yang, Q. & Zhu, S. 2009. Effect of tool geometry on static strength of friction stir spot-welded aluminum alloy. *International Journal of Machine Tools and Manufacture* 49(2): 142–148.

Bozzi, S., Helbert-Etter, A.L., Baudin, T., Klosek, V., Kerbiguet, J.G. & Criqui, B. 2010. Influence of FSSW parameters on fracture mechanisms of 5182 aluminium welds. *Journal of Materials Processing Technology* 210(11): 1429–1435.

Buffa, G., Fratini, L., Schneider, M. & Merklein, M. 2013. Micro and macro mechanical characterization of friction stir welded Ti-6Al-4V lap joints through experiments and numerical simulation. *Journal of Materials Processing Technology* 213(12): 2312–2322.

Dung-An Wang & S.-C. Lee. 2007. Microstructures and failure mechanisms of friction stir spot welds of aluminum 6061-T6 sheets. *Journal of Materials Processing Technology* 186(1): 291–297.

Garg, A. & Bhattacharya, A. 2017. On lap shear strength of friction stir spot welded AA6061 alloy. *Journal of Manufacturing Processes* 26: 203–215.

Gibson, B.T., Lammlein, D.H., Prater, T.J., Longhurst, W.R., Cox, C.D., Ballun, M.C., Dharmaraj, K.J., Cook, G.E. & Strauss, A.M. 2014. Friction stir welding: Process, automation, and control. *Journal of Manufacturing Processes* 16(1): 56–73.

Gui-ju Zhang, Cai-yuan Xiao & Olantunji Oladimeji Ojo. 2021. Dissimilar friction stir spot welding of AA2024-T3/AA7075-T6 aluminum alloys under different welding parameters and media. *Defence Technology* 17(2): 531–544.

Hunt, F., Badarinarayan, H. & Okamoto, K. 2006. Design of experiments for friction stir stitch welding of aluminum alloy 6022-T4: Friction stir welding of aluminum for automotive applications (3). *SAE Technical Papers* 142: 84–93.

Ilangovan, M., Rajendra, B.S. & Balasubramanian, V. 2015. Effect of tool pin profile on microstructure and tensile properties of friction stir welded dissimilar AA6061–AA5086 aluminium alloy joints. *Defence Technology* 11(2): 174–184.

Khan, N.Z., Siddiquee, A.N., Khan, Z.A. & Mukhopadhyay, A.K. 2017. Mechanical and microstructural behavior of friction stir welded similar and dissimilar sheets of AA2219 and AA7475 aluminium alloys. *Journal of Alloys and Compounds* 695: 2902–2908.

Lee, S.H., Lee, D.M. & Lee, K.S. 2017. Process optimisation and microstructural evolution of friction stir spot-welded Al6061 joints. *Materials Science and Technology (United Kingdom)* 33(6): 719–730.

Mamgain, A., Singh, V. & Pratap Singh, A. 2023. Influence of welding parameters on mechanical property during friction stir welded joint on aluminium alloys: A review. *Jurnal Kejuruteraan* 35(1): 13–28.

Mitlin, D., Radmilovic, V., Pan, T., Chen, J., Feng, Z. & Santella, M.L. 2006. Structure–properties relations in spot friction welded (also known as friction stir spot welded) 6111 aluminum. *Materials Science and Engineering A* 441(1): 79–96.

Nasir, T., Kalaf, O. & Asmael, M. 2021. Effect of rotational speed, and dwell time on the mechanical properties and microstructure of dissimilar aa5754 and aa7075-t651 aluminum sheet alloys by friction stir spot welding. *Medziagotyra* 27(3): 308–312.

Norfazilah Mohd Selamat, Amirhossein Baghdadi, Zainuddin Sajuri, Amir Hossein Kokabi & Syarif Junaidi. 2018. Effect of rolling on strength of friction stir welded joint of aluminium alloys. *Jurnal Kejuruteraan* 1(6): 9–15.

Ojo, O.O., Taban, E. & Kaluc, E. 2015. Friction stir spot welding of aluminum alloys: A recent review. *Materials Testing* 57(7–8): 609–627.

Pabandi, H.K., Jashnani, H.R. & Paidar, M. 2018. Effect of precipitation hardening heat treatment on mechanical and microstructure features of dissimilar friction stir welded AA2024-T6 and AA6061-T6 alloys. *Journal of Manufacturing Processes* 31: 214–220.

Paidar, M. & Sarab, M.L. 2016. Friction stir spot welding of 2024-T3 aluminum alloy with SiC nanoparticles. *Journal of Mechanical Science and Technology* 30(1): 365–370.

Paidar, M., Khodabandeh, A., Sarab, M.L. & Taheri, M. 2015. Effect of welding parameters (plunge depths of shoulder, pin geometry, and tool rotational speed) on the failure mode and stir zone characteristics of friction stir spot welded aluminum 2024-T3 sheets. *Journal of Mechanical Science and Technology* 29(11): 4639–4644.

Paidar, M., Vaira Vignesh, R., Moharrami, A., Ojo, O.O., Jafari, A. & Sadreddini, S. 2020. Development and characterization of dissimilar joint between AA2024-T3 and AA6061-T6 by modified friction stir clinching process. *Vacuum* 176: 109298.

Paidar, M., Vignesh, R.V., Khorram, A., Ojo, O.O., Rasoulpouraghdam, A. & Pustokhina, I. 2020. Dissimilar modified friction stir clinching of AA2024-AA6061 aluminum alloys: Effects of materials positioning. *Journal of Materials Research and Technology* 9(3): 6037–6047.

Pathak, N., Bandyopadhyay, K., Sarangi, M. & Panda, S.K. 2013. Microstructure and mechanical performance of friction stir spot-welded aluminum-5754 sheets. *Journal of Materials Engineering and Performance* 22(1): 131–144.

Qingzhao Wang, Zhixia Zhao, Yong Zhao, Keng Yan & Hao Zhang. 2015. The adjustment strategy of welding parameters for spray formed 7055 aluminum alloy underwater friction stir welding joint. *Materials and Design* 88: 1366–1376.

Rodriguez, R.I., Jordon, J.B., Allison, P.G., Rushing, T. & Garcia, L. 2015. Microstructure and mechanical properties of dissimilar friction stir welding of 6061-to-7050 aluminum alloys. *Materials and Design* 83: 60–65.

Sadeghi, B., Abbasi, H., Atapour, M., Shafiee, S., Cavaliere, P. & Marfavi, Z. 2020. Friction stir spot welding of TiO2 nanoparticle-reinforced interstitial free steel. *Journal of Materials Science* 55(26): 12458–12475.

Sekhar, S.R., Chittaranjandas, V., Govardhan, D. & Karthikeyan, R. 2018. Effect of tool rotational speed on friction stir spot welded AA5052-H38 aluminum alloy. *Materials Today: Proceedings* 5(2): 5536–5543.

Van-Xuan Tran, Pan, J. & Pan, T.Y. 2008. Effects of processing time on strengths and failure modes of dissimilar spot friction welds between aluminum 5754-O and 7075-T6 sheets. *Journal of Materials Processing Technology* 209(8): 3724–3739. DOI:10.1016/j.jmatprotec.2008.08.

Yazdipour, A. & Heidarzadeh, A. 2016. Effect of friction stir welding on microstructure and mechanical properties of dissimilar Al 5083-H321 and 316L stainless steel alloy joints. *Journal of Alloys and Compounds* 680: 595–603.

Zhaohua Zhang, Jialong Zhang, Guang Zhou, Xiadong Xu, Binilan Zou & Xinqi Yang. 2011. Effect of welding parameters on microstructure and mechanical properties of friction stir spot welded 5052 aluminum alloy. *Mater. Des. Materials and Design* 32(8–9): 4461–4470.

Zheng Ming Su, R.-Y. He, Pai-Chen Lin & Kexin Dong. 2014. Fatigue analyses for swept friction stir spot welds in lap-shear specimens of alclad 2024-T3 aluminum sheets. *International Journal of Fatigue* 61: 129–140.

Zhenlei Liu, Kang Yang & Dejum Yan. 2019. Refill friction stir spot welding of dissimilar 6061/7075 aluminum alloy. *High Temperature Materials and Processes* 38: 69–75.

Zhikang Shen, Xinqi Yang, Zhaohua Zhang, Lei Cui & Yuhuan Yin. 2013. Mechanical properties and failure mechanisms of friction stir spot welds of AA 6061-T4 sheets. *Materials and Design* 49: 181–191.

Zhongjie Yan, Xuesong Liu & Hongyuan Fang. 2016. Effect of sheet configuration on microstructure and mechanical behaviors of dissimilar Al–Mg–Si/Al–Zn–Mg aluminum alloys friction stir welding joints. *Journal of Materials Science and Technology* 32(12): 1378–1385.